

# Temperature dependence of the Kondo resonance and its satellites in CeCu<sub>2</sub>Si<sub>2</sub>

F. Reinert,\* D. Ehm, S. Schmidt, G. Nicolay, and S. Hüfner

*Universität des Saarlandes, Fachrichtung 7.2 — Experimentalphysik, 66041 Saarbrücken, Germany*

J. Kroha

*Institut für Theorie der Kondensierten Materie, Universität Karlsruhe, Engesserstr. 7, 76128 Karlsruhe, Germany*

O. Trovarelli and C. Geibel

*Max-Planck Institute for Chemical Physics of Solids, Nöthnitzer Str. 40, 01187 Dresden, Germany*

(Dated: November 4, 2018)

We present high-resolution photoemission spectroscopy studies on the Kondo resonance of the strongly-correlated Ce system CeCu<sub>2</sub>Si<sub>2</sub>. Exploiting the thermal broadening of the Fermi edge we analyze position, spectral weight, and temperature dependence of the low-energy 4f spectral features, whose major weight lies above the Fermi level  $E_F$ . We also present theoretical predictions based on the single-impurity Anderson model using an extended non-crossing approximation (NCA), including all spin-orbit and crystal field splittings of the 4f states. The excellent agreement between theory and experiment provides strong evidence that the spectral properties of CeCu<sub>2</sub>Si<sub>2</sub> can be described by single-impurity Kondo physics down to  $T \approx 5$  K.

PACS numbers: 71.27.+a 71.28.+d 79.60.-i 71.10.-w

Many of the salient properties of intermetallic rare earth compounds originate from strong electronic correlations in the rare earth 4f orbitals. The hybridization with the conduction electron continuum leads to complex low-temperature behavior, summarized by the term Kondo scenario [1]. It includes quenching of the 4f magnetic moments below the Kondo temperature  $T_K$ , a strong enhancement of thermodynamic quantities like the magnetic susceptibility and the specific heat. The latter is ascribed to an enhanced electron density of states (DOS) at the Fermi energy  $E_F$ , the Kondo resonance (KR). In lattice systems, below a so-called lattice coherence temperature  $T^*$ , the transport properties [2] can often be described by the assumption of *propagating* quasiparticles with an effective mass enhancement of  $m_e^*/m_e = 10^2$  to  $10^3$ . The coherence temperature  $T^*$  can be in the same range as  $T_K$  [3]. Several of these heavy Fermion systems [4] undergo a magnetic ordering transition at low temperature  $T$ , become paramagnetic insulators (Kondo insulators) or even superconducting, like CeCu<sub>2</sub>Si<sub>2</sub> [5], where  $T_K \approx 4.5$  K to 10 K [6, 7] and  $T^* \approx 10$  K [3]. In order to understand the interplay between local moment quenching and lattice coherence and ordering effects it is essential to know to what extent the system is described by local Kondo physics. However, it has been notoriously difficult to directly investigate the KR experimentally. In fact, the Kondo scenario as the origin of the 4f DOS enhancement in Ce-based compounds has repeatedly been disputed in the literature (see [8] and references therein), mainly because the enhancement can still be seen at temperatures almost two orders of magnitude above  $T_K$ .

There exist three established, spectroscopic methods to investigate the spectral function close to the Fermi energy, photoemission (PES), inverse photoemis-

sion (IPES) and scanning tunneling spectroscopy (STS). In the case of Ce compounds the 4f occupation is close to unity ( $4f^1$ ), the Kondo temperature lies in the range  $T_K \approx 1, \dots, 1000$  K [4], and the KR has its maximum *above*  $E_F$ . The difficulty in observing the KR lies in the limited IPES energy resolution of  $O(100$  meV), whereas PES has, in general, merely access to the tail of the KR below  $E_F$  and STS [9] probes the local 4f spectrum only indirectly by tunneling into the conduction states [10].

In this Letter we present a careful analysis of high-resolution PES data close to the Fermi level, which allows to acquire information of the spectral function above the Fermi level. We restrict ourselves here to the heavy fermion compound CeCu<sub>2</sub>Si<sub>2</sub>, although experimental method and data analysis [11] have also been successfully applied to other Ce intermetallics [12]. A comparison with calculations of the 4f spectral function, based on the single-impurity Anderson model (SIAM) including spin-orbit (SO) as well as crystal field (CF) splitting of the local orbitals, shows striking agreement between experiment and theory. In particular, we explain the temperature dependence of the spectral features up to  $T = 200$  K.

The PES experiments have been performed using a SCIENTA SES 200 analyzer and a monochromatized GAMMADATA VUV-lamp at photon energies of  $h\nu = 21.2$  eV (He I) and  $h\nu = 40.8$  eV (He II). A description of the experimental setup and the calibration of the experimental parameters for the high-resolution measurements, like  $E_F$ , sample temperature  $T$ , and energy resolution  $\Delta E$ , can be found in more detail in Ref. [13]. The poly-crystalline samples were cleaved *in situ* at low  $T$  to prepare clean surfaces. Because of the high surface reactivity of rare-earth compounds [14] the duration of a

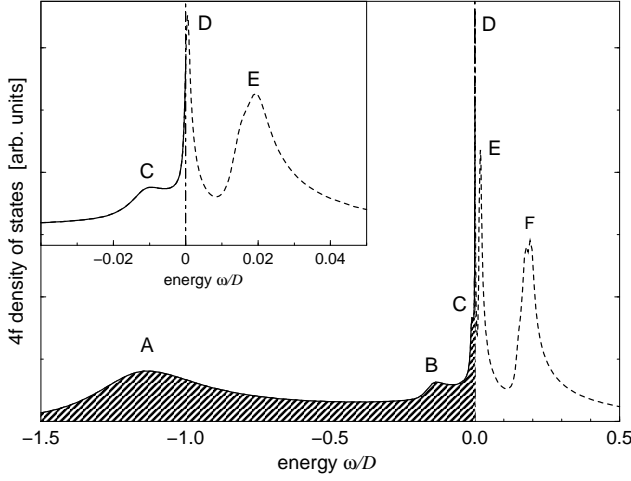


FIG. 1: Theoretical 4f spectral function from calculations based on the SIAM using the NCA for  $T = 11$  K and model parameters as in Fig. 3. The hatched region is the occupied part of the spectrum. Energies are given in units of the half band width  $D = E_F$ . The inset shows the near- $E_F$  region. The spectral features A – F are explained in the text. The two-electron state  $f^2$  lies far outside the displayed energy range at  $\approx U + \epsilon_{f1}$ .

measurement was kept less than about 12 h.

In  $\text{CeCu}_2\text{Si}_2$  the 7 spin-degenerate 4f levels are split by SO coupling into a total angular momentum  $J = 5/2$  sextet and an excited  $J = 7/2$  octet. These are, in turn, CF split into 3 and 4 Kramers degenerate doublets, respectively. Thus, the single-impurity system is described by the multi-orbital Anderson Hamiltonian

$$H = H_0 + \sum_{m\sigma} \epsilon_{fm} f_{m\sigma}^\dagger f_{m\sigma} + \sum_{\vec{k}m\sigma} (V_{\vec{k}m} c_{\vec{k}\sigma}^\dagger f_{m\sigma} + \text{h.c.}) + \frac{U}{2} \sum_{(m\sigma) \neq (m'\sigma')} f_{m\sigma}^\dagger f_{m\sigma} f_{m'\sigma'}^\dagger f_{m'\sigma'}, \quad (1)$$

where  $H_0 = \sum_{\vec{k}\sigma} \epsilon_{\vec{k}} c_{\vec{k}\sigma}^\dagger c_{\vec{k}\sigma}$  describes the conduction band with dispersion  $\epsilon_{\vec{k}}$  and creation operators  $c_{\vec{k}\sigma}^\dagger$  for electrons with spin  $\sigma$ .  $\epsilon_{fm} < E_F$ ,  $m = 1, \dots, 7$ , are the SO and CF split 4f single-particle levels with the corresponding creation operators  $f_{m\sigma}^\dagger$ . The hybridization matrix elements  $V_{\vec{k}m}$  lead to an effective coupling matrix between 4f states,  $\Gamma_{mn} = \pi \sum_{\vec{k}} V_{m\vec{k}}^* A_{\vec{k}}(\omega) V_{\vec{k}n}$ , where  $A_{\vec{k}}(\omega)$  is the conduction electron spectral function. The local Coulomb repulsion, known from IPES [15, 16], is substantially larger than  $|\epsilon_{f1}|$  and, hence, effectively suppresses any double occupancy of the Ce 4f levels ( $U \rightarrow \infty$ ). In the multi-orbital system the Kondo temperature is given by  $T_K \approx \sqrt{2J\epsilon_F} \exp[-1/(2N(0)J)]$ , where  $N(0)$  is the conduction electron DOS at the Fermi level and the Kondo coupling  $J$  is obtained from a Schrieffer–Wolff

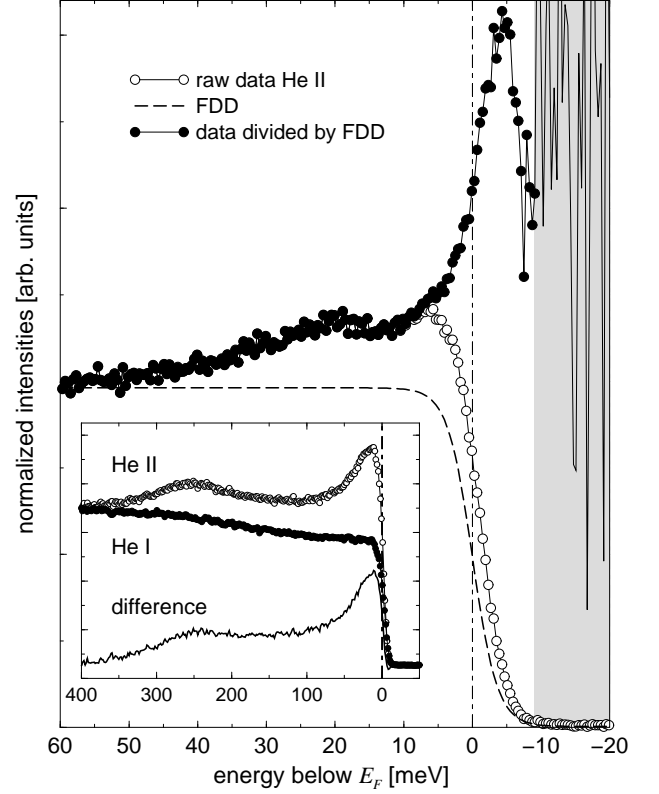


FIG. 2: Photoemission spectrum of  $\text{CeCu}_2\text{Si}_2$  ( $h\nu = 40.8$  eV, He II). Open circles represent the raw data close to the Fermi level, including the tail of the KR and the low-energy CF excitations at approximately 21 meV ( $\Delta E = 6$  meV,  $T = 11$  K). Filled circles represent the raw data divided by the experimentally broadened FDD (see text). The shaded area marks the unreliable spectral range above  $5k_B T$ . The inset shows an extended energy range (measured with  $\Delta E \sim 13$  meV,  $T = 17$  K) including the spin-orbit ( $J=7/2$ ) excitation at  $\approx 270$  meV below  $E_F$  and the non-4f background as determined using He I ( $h\nu = 21.2$  eV) radiation.

transformation including the CF and SO states as

$$J = \frac{|\sum_{\vec{k}} V_{\vec{k}1}|^2}{\left| \epsilon_{f1} + \sum_{m>1} \frac{|\sum_{\vec{k}} V_{\vec{k}m}|^2}{\epsilon_{fm} - \epsilon_{f1}} \right|}. \quad (2)$$

It is seen that  $J$ , and hence  $T_K$ , is enhanced due to coupling to the CF and SO split 4f states.

To achieve a detailed comparison with experimental results, we have calculated the 4f spectral function of the model Eq. (1) using the non-crossing approximation (NCA) [17, 18] including all CF and SO excitations. The NCA is known to reliably describe the low-temperature scale  $T_K$  and the position, the spectral weight and the life-time broadening of the peaks in the local spectral density down to  $T \approx 0.1 T_K$  [17]. The spectrum has generically six distinct features as shown in Fig. 1 (A–F). They can be understood as follows: At low  $T$  the occupation of the lowest 4f level is close to unity ( $n_{f1} \lesssim 1$ ), while

all other single-particle 4f states are essentially empty ( $n_{fm} \approx 0$ ,  $m = 2, \dots, 7$ ) because of the strong Coulomb repulsion  $U$ . Hence, the broad  $4f^1 \rightarrow 4f^0$  ionization peak (A) with a full width at half maximum (FWHM) of  $\Gamma \approx \sum_m \Gamma_{1m}$  corresponds to the lowest single-particle level  $\varepsilon_{f1}$ . Resonant spin flip scattering of electrons at the Fermi energy induces the narrow Kondo resonance (D) of width  $\sim k_B T_K$ , somewhat shifted above  $E_F$  due to level repulsion from the single-particle levels  $\varepsilon_{fm} < E_F$ . The SO and the CF satellite peaks appear in pairs (B, F) and (C, E), respectively. They arise from virtual transitions from the ground state into the (empty) excited SO (F) and CF (E) states and vice versa (B and C). The positions of the satellite peak pairs are, therefore, approximately symmetrical about  $E_F$ . However, while the features above  $E_F$  have significant spectral weight, those below  $E_F$  appear merely as weak shoulders. This is because the transition probabilities carry a detailed balance factor  $w = n^i(1 - n^f)$ , where  $n^i$  ( $n^f$ ) is the occupation number of the 4f orbital in the initial (final) state, i.e.  $w$  is large for the excitations E, F, but small for the transitions B, C.

As  $n^i$ ,  $n^f$  are controlled both by  $T$  and  $U$ , the CF and SO satellites are signatures of strong correlations and are  $T$ -dependent. All these features are well described by the NCA (Fig. 1). We note in passing that similar spectra should be observed in multilevel quantum dots in the Kondo regime.

In order to identify the low-energy features in experimental spectra as due to the physics of the single-impurity Anderson model (Eq. 1), it is highly desirable to gain access to the sharp resonances D, E above  $E_F$ . A typical high-resolution spectrum on  $\text{CeCu}_2\text{Si}_2$  is shown in Fig. 2, measured at  $T = 11$  K with an energy resolution of  $\Delta E = 6$  meV. The ionization peak A (not shown) appears at a binding energy of  $\approx 2$  eV below  $E_F$ , the SO satellite B at  $\approx 270$  meV. Fig. 2 shows the near- $E_F$  region with the tail of the KR and a distinct spectral feature at about 21 meV, which can be assigned to the CF splitting of the  $J = 5/2$  4f levels [19]. In this plot the spectral intensity at energies of a few meV above  $E_F$  and higher is completely suppressed by the Fermi-Dirac distribution (FDD). IPES experiments performed on similar systems do not resolve the KR and its satellite excitations expected above  $E_F$ , but show only one broad structure near  $E_F$  and a second one at much higher energies, corresponding to the doubly occupied IPES final state  $4f^1 \rightarrow 4f^2$  [15, 16].

Greber *et al.* [20] have demonstrated that a careful analysis of PES data based on a division by the respective FDD allows to investigate the spectral function up to energies of approximately  $5k_B T$  above  $E_F$ , provided that the noise of the data and the experimental broadening are small enough. We applied this procedure to the spectrum in Fig. 2, where we divided the raw spectrum by the FDD at  $T = 11$  K convoluted with the spectrom-

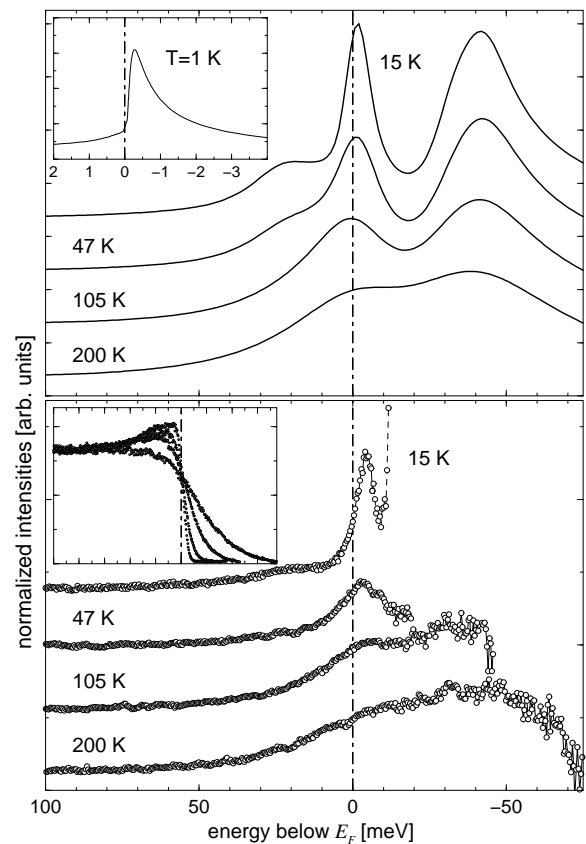


FIG. 3: Upper panel: Theoretical  $T$  dependence of the 4f spectral function of  $\text{CeCu}_2\text{Si}_2$ . The inset shows the calculated spectrum below  $T_K$  (see text). Used model parameters:  $\varepsilon_{f1} = -2.4$  eV,  $E_F = 4$  eV, CF splittings of the  $J = 5/2$  sextet  $\Delta_{CF} = 30$  meV and 36 meV, SO splitting  $\Delta_{SO} = 270$  meV, hybridization  $V = 200$  meV. Lower panel: Photoemission spectra for  $T = 15$  K, 47 K, 105 K, and 200 K. The experimental spectra, divided by the FDD, are clipped on the high energy side at  $\approx 5k_B T$ . The inset shows the data on the same energy scale prior to the division. All spectra are normalized to the same intensity at  $\approx 100$  meV and offset for clarity.

ter function, described by a Gaussian of full width at half maximum (FWHM)  $\Delta E = 6$  meV. Obviously there appears a narrow peak with a FWHM of 6 meV and a maximum at about 3 meV above  $E_F$ . This is sufficiently below  $5k_B T \approx 7$  meV at which energy the scatter of the data gets large due to the exponential increase of the inverse FDD. The spectrum of the CF satellite at  $\approx 21$  meV below  $E_F$  remains unchanged by this procedure. It should be mentioned that the described procedure is not exact and therefore can lead to artifacts (of the order of  $\Delta E$ ) if the temperature broadening is comparable with the energy resolution. However, in the present case this is only relevant for the 11 K-spectrum which appears slightly shifted away from  $E_F$ .

In the following we analyze the  $T$  dependence of the near- $E_F$  spectral features. Fig. 3, lower panel, shows

the experimental data at several temperatures, divided by the broadened FDD as described above. The upper panel of Fig. 3 displays the NCA spectral functions for the same temperatures. The model parameters, i.e. the single-particle energies  $\epsilon_{fm}$  and the hybridization strengths  $\Gamma_{mm'}$ , have been taken from independent experimental measurements where possible [19, 22] and have only slightly been adjusted (see caption of Fig. 3) to get optimal quantitative agreement with our experimental results. The experimentally observed temperature dependence of the spectra is accurately described by the theoretical simulations, and a comparison allows to identify the origin of the various spectral features: As already seen in Fig. 2 at low  $T$  ( $T = 15$  K) the KR at  $E_F$  appears as a narrow line with a FWHM of about 6 meV. Due to the given energy resolution of  $\Delta E = 6$  meV the intrinsic linewidth of the Kondo resonance must be much smaller than  $\Delta E$  at low temperatures. In order to estimate  $T_K$  from the data we have determined the model parameters to fit the experimental results at their respective  $T$  and then calculated the spectrum at  $T = 0.1 T_K \approx 1$  K (inset of Fig. 2, upper panel), i.e. close to the unitarity limit which is not directly reachable in the experiment.  $T_K$  was then determined from the peak width of this theoretical low- $T$  spectrum as  $T_K \approx 6$  K. This result is in remarkable agreement with thermodynamic bulk measurements [5, 6, 7], considering especially that the spectral function — and therewith  $T_K$  — as measured by surface sensitive PES might be modified by surface effects, as pointed out by several authors [14, 21, 23]. Towards higher  $T$ , the line width of the KR increases, while the maximum intensity becomes smaller and the distinction of KR and CF satellite is successively smeared out. At  $T = 200$  K and above the thermal broadening of the FDD is large enough for PES to have access to the CF excitations at  $\sim 40$  meV. At these elevated  $T$  the KR has disappeared as a separate peak, and the enhanced 4f DOS near  $E_F$  is rather due to the CF excitations which are broadened and positioned somewhat above  $E_F$ , as seen in Fig. 3. Thus, the persistence of an enhanced DOS at the Fermi level even at room temperature, despite a substantially lower  $T_K$ , is naturally explained within the SIAM in combination with CF excited states.

In conclusion we have demonstrated that high resolution photoemission spectroscopy gives detailed access to the spectral function of heavy Fermion Ce compounds and allows to investigate the temperature dependence of the Kondo resonance. Within an energy range of  $5k_B T$  above the Fermi level several structures can be resolved, whose origin and temperature dependence are consistently described within the single-impurity Anderson model. This excellent agreement provides strong evidence that the 4f photoemission spectra of CeCu<sub>2</sub>Si<sub>2</sub> are an immediate consequence of single-impurity Kondo

physics, although the Kondo local moment quenching and lattice coherence effects occur on similar energy scales ( $T^* \approx T_K$ ). In particular, the Kondo resonance could be unambiguously identified, with a Kondo temperature in reasonable agreement with estimates from thermodynamic measurements. The persistence of an enhanced density of states even at room temperature is explained by the presence of crystal field excited states close to the Fermi energy.

We wish to thank P. Wölfle for stimulating discussions. This work was supported by the Deutsche Forschungsgemeinschaft (grant nos. HU149-19-1, HU149-17-4) and by Sonderforschungsbereiche SFB 277 and SFB 195.

---

\* corresponding author. Email: friedel@mx.uni-saarland.de

- [1] For a comprehensive introduction see A. C. Hewson, *The Kondo Problem to Heavy Fermions* (Cambridge University Press, 1993).
- [2] P. Fulde, *Electron Correlations in Molecules and Solids*, Springer Series in Solid-State Sciences **100** (Springer, Berlin-Heidelberg-New York, 1995).
- [3] G. Knebel et al., Phys. Rev. B **53**, 11586 (1996).
- [4] K. A. Gschneidner, Jr. and L. R. Eyring, eds., *Handbook on the Physics and Chemistry of Rare Earths*, (North-Holland, Amsterdam–New York–Oxford, 1982–1999).
- [5] F. Steglich et al., Phys. Rev. Lett. **43**, 1892 (1979).
- [6] C. D. Bredl et al., Phys. Rev. Lett. **52**, 1982 (1984).
- [7] S. Horn et al., Phys. Rev. B. **23**, 3171 (1981).
- [8] A. J. Arko et al., in Ref. [4] **26**, chap. 172, pp. 265–382 (1999).
- [9] J. Li, W.-D. Schneider, R. Berndt, and B. Delley, Phys. Rev. Lett. **80**(13), 2893 (1998); Madhavan et al., Science **280**, 567 (1998).
- [10] O. Újsághy, J. Kroha, L. Szunyogh and A. Zawadowski, Phys. Rev. Lett. **85**, 2557 (2000).
- [11] H. Kumigashira et al. Phys. Rev. Lett. **82**, 1943 (1999).
- [12] D. Ehm, Ph.D. thesis, Universität des Saarlandes, Saarbrücken (2001), to be published.
- [13] F. Reinert et al., Phys. Rev. B **63**, 115415 (2001).
- [14] F. Reinert et al., Phys. Rev. B. **58**, 12808 (1998).
- [15] M. Grioni et al., Phys. Rev. B **55**, 2056 (1997).
- [16] K. Kanai et al., Phys. Rev. B **60**, R9900 (1999).
- [17] N. E. Bickers, D. L. Cox, and J. W. Wilkins, Phys. Rev. B. **36**(4), 2036 (1987).
- [18] For an efficient implementation see T. A. Costi, J. Kroha, and P. Wölfle, Phys. Rev. B **53**, 1850 (1996).
- [19] E. A. Goremychkin, and R. Osborn, Phys. Rev. B. **47**(21), 14280 (1993).
- [20] T. Greber, T. J. Kreutz, and J. Osterwalder, Phys. Rev. Lett. **79**(22), 4465 (1997).
- [21] M. Garnier et al., Phys. Rev. Lett. **78**(21), 4127 (1997).
- [22] J.-S. Kang et al., Phys. Rev. B. **41**, 6610 (1990).
- [23] A. Sekiyama et al., Nature **403**, 396 (2000).